A model-data fusion approach to analyse carbon dynamics in managed grasslands

Vasileios Myrgiotis[a], Emanuel Blei[a], Rob Clement[a], Stephanie K. Jones[b], Ben Keane[d], Mark A. Lee[e], Peter E. Levy[c], Robert M. Rees[b], Ute M. Skiba[c], Thomas Luke Smallman[a], Sylvia Toet[d], Mathew Williams[a]

[a]*School of GeoSciences and National Centre for Earth Observation, University of Edinburgh, Edinburgh EH9 3JN, UK*
[b]*Scotland's Rural College, King's Buildings, West Mains Road, Edinburgh, EH9 3JG, UK*
[c]*Centre for Ecology and Hydrology, Edinburgh, Bush Estate, Penicuik, Midlothian, EH26 0QB, UK*
[d]*Department of Environment and Geography, Wentworth Way, University of York, Heslington, York, YO10 5NG, UK*
[e]*Natural Capital and Plant Health, Royal Botanic Gardens Kew, Richmond, TW9 3AB, UK*

Abstract

Grasslands are an important component of the global carbon (C) cycle, with a strong potential for C sequestration. However, an improved capacity to quantify grassland C stocks and monitor their variation in space and time, particularly in response to management, is needed in order to conserve and enhance grassland C reservoirs. To meet this challenge we outline and test here an approach to combine C cycle modelling with observational data. We implemented an intermediate complexity model, DALEC-Grass, within a probabilistic model-data fusion (MDF) framework, CARDAMOM, at two managed grassland sites (Easter Bush and Crichton) in the UK. We used 3 years (Easter Bush, 2002-2004) of management data and observations of leaf area index (LAI) and Net Ecosystem Exchange (NEE) from eddy covariance to calibrate the distributions of model parameters. Using these refined distributions, we then assimilated the remaining 7 years (Easter Bush, 2005-2010 and Crichton, 2015) of LAI observations and evaluated the simulated NEE, above and below-ground biomass and other C fluxes against independent data from the two grasslands. Our results show that fusing model predictions with LAI observations allowed the CARDAMOM MDF system to diagnose the effects of grazing and cutting realistically. The overlap of MDF-predicted

and measured NEE (both sites) and ecosystem respiration (Easter Bush) was 92% and 83% respectively while the correlation coefficient (r) was 0.79 for both variables. This study lays the foundation for using MDF with satellite data on LAI to produce the spatially and temporally-resolved estimates of C cycling needed in shaping and monitoring the implementation of relevant policies and farm-management decisions.

Keywords: UK grasslands, primary production, carbon sequestration, model-data fusion

---

Ecosystem carbon accounting abbreviations

Gross Primary Production : GPP
Autotrophic Respiration : AR
Heterotrophic Respiration : HR
Ecosystem Respiration : ER = AR + HR
Net Primary Production : NPP = GPP - AR
Net Ecosystem Exchange : NEE = ER - GPP
Net Ecosystem Production : NEP = GPP - ER

1. Introduction

Grasslands cover a third of the earth's surface and are a major component of the terrestrial biosphere's carbon (C) cycle and a major contributor to global annual fluxes and C stores (Hungate et al., 2017; Friedlingstein et al., 2019; Sollenberger et al., 2019). Temperate grasslands, because of edaphoclimatic conditions and their botanical composition, can transfer and accumulate C in their soils more efficiently than grasslands in warmer and drier regions (Gibson, 2010). Based on this premise, and considering the rise in atmospheric CO_2 concentration, European grasslands have the potential for increased CO_2 sequestration (Chang et al., 2017). Estimates of grassland C balance and its variation in space and time are essential for shaping evidence-informed climate policies and monitoring progress on Nationally Determined Contributions (NDCs) following the Paris agreement (De Oliveira Silva et al., 2018). Livestock grazing and grass harvesting affect grassland C stocks, typically removing >50% of vegetation C on an annual basis (Erb et al., 2018). In addition to sustaining livestock farming by providing biomass energy to livestock directly from grazing or as fodder, vegetation also provides inputs to the soil C pool in the form of litter and exudates, as well as indirectly from excrement produced by grazers (Soussana and Lemaire, 2014; Chen et al., 2015; Conant et al., 2017; Abdalla et al., 2018). Because of its dynamic nature, the C balance of vegetation in managed grasslands (i.e. assimilation, allocation, removal and loss) is complex and challenging to monitor and assess.

Detailed, continuous measurements of the C dynamics of grasslands are limited to a few sites globally. Computational approaches are therefore used to extrapolate observed relationships across landscapes. Such computational methods include (1) statistical models that relate climate data and selected

national statistics to grassland productivity and removals (e.g. Smit et al., 2008; Herrero et al., 2013; Qi et al., 2017, 2018); (2) process-based grassland models that simulate C uptake and turnover (e.g. Vuichard et al., 2007; Chang et al., 2013; Snow et al., 2014; Chang et al., 2015; Kipling et al., 2016; Rolinski et al., 2018; Puche et al., 2019; Sándor et al., 2020; van Oijen et al., 2020); and (3) processed earth observation (EO) data that map and track key ecological variables, such as leaf area index (e.g. Franke et al., 2012; Dusseux et al., 2014; Asam et al., 2015; Xu and Guo, 2015; Ali et al., 2016; Gómez Giménez et al., 2017; Punalekar et al., 2018). Each method has its strengths and weaknesses. Statistical approaches are strongly grounded on measured data but have low sensitivity to the spatial and temporal variation of system drivers (e.g. climate, management) and have limited explanatory depth (Smit et al., 2008). Process models describe most of the underlying biogeochemical processes, which gives them greater explanatory depth than purely statistical approaches and the capacity to explore the consequences of different management and soil-climate conditions. But process models require observational data for parameter calibration and output error evaluation (Ma et al., 2015; Ehrhardt et al., 2017). Model-based studies tend to present deterministic results, ignoring the role of uncertainties around model inputs, parameters and structure, and observed data (Smith et al., 2012; Kipling et al., 2016). Earth observations increasingly provide snapshots at high temporal and spatial resolution on certain drivers and proxies of C dynamics (e.g. vegetation structure, soil moisture). But these products do not consider the full C budget, particularly below ground, nor diagnose how grassland ecosystems C storage evolves (Ali et al., 2016).

Model-data fusion (MDF) is a hybrid approach that combines aspects of the three aforementioned computational approaches (Raupach et al., 2005). MDF uses probabilistic methods to calibrate model parameters and/or to quantify model predictive uncertainty (Gottschalk et al., 2007; Patenaude et al., 2008; Ben Touhami and Bellocchi, 2015; Oenema et al., 2015; van Oijen, 2017). From an ecosystem modelling perspective, MDF can be understood as a framework in which model parameter distributions are calibrated according to a set of observations (observed data assimilation) and model output uncertainty is quantified. The behaviour of simulated fluxes and pools is constrained according to certain rules. For instance, ancillary data from national statistics, land surveys and scientific literature can be integrated in a MDF framework. The strong linkage to observations means that MDF is suitable for quantifying the existing situation and for explaining the

mechanisms that underlie the functioning of a grassland. Model-data fusion can accommodate models of varying complexity (e.g number of parameters, modules, calculation nodes) but increasing complexity increases the computational cost and can reduce the robustness of the MDF process. The MDF approach has been used in studies focusing on various aspects of terrestrial ecosystem C dynamics (e.g. productivity, biomass, fire emissions) in the past (Wang et al., 2009; Fox et al., 2009; Keenan et al., 2012; Kuppel et al., 2014; Xiao et al., 2014; Kuppel et al., 2014; Bloom and Williams, 2015; Peylin et al., 2016; Smallman et al., 2017; Scholze et al., 2017; Peaucelle et al., 2019). Model-data fusion is actively benefiting from the increasing quality and range of EO data and can be used to monitor terrestrial ecosystem C balance at various spatial and temporal scales (Guo et al., 2014; Bloom et al., 2016; Ramapriyan and Murphy, 2017; Chen and Wang, 2018).

Here, for the first time to our knowledge, we apply MDF to analyse ecosystem C cycling in managed grasslands. Previous probabilistic model-based studies have focused on plant functional type identification and have not considered the role of management on C cycling (Kuppel et al., 2014; Peylin et al., 2016; Peaucelle et al., 2019). In this study, we present a development of the Data Assimilation Linked Ecosystem Carbon model (DALEC) that is tailored for use in MDF for grasslands (DALEC-Grass). DALEC is a C-budget model that is integrated into the Carbon Data Model Framework (CARDAMOM) (Bloom and Williams, 2015; Bloom et al., 2016; Smallman et al., 2017). DALEC and the CARDAMOM MDF framework have been used before in MDF studies on forests and croplands (Revill et al., 2016; Smallman et al., 2017). The aim of the present study is to demonstrate MDF with DALEC-Grass and test its ability to quantify C dynamics in grasslands under variable grazing and cutting regimes. As a first step, we calibrate the distribution of DALEC-Grass parameters using 3 years of measured data on leaf area index (LAI) and net ecosystem exchange (NEE) from a grassland in eastern Scotland (UK). LAI data are routinely estimated from EO systems at fine spatial ($<$ha) and temporal resolutions ($\approx$ days). Therefore, time series of satellite LAI data have the potential to inform and constrain grassland models effectively at sub-field scales and during critical growth changes and management interventions. As a second step, we tested this assumption by evaluating our model's predictive skill when a limited number of field-measured LAI data are assimilated through the CARDAMOM MDF framework. We assess the model's performance by comparing its outputs to independent eddy flux data on NEE of CO_2, above and below-ground

biomass and soil respiration from chambers. Six additional years of data from the core study site and one year of data from another UK site are used for the validation process. The materials and methods section describes the DALEC-Grass model, the CARDAMOM framework, the characteristics of the grassland sites that are modelled and the methodology that is followed. Finally, we discuss the potential for DALEC-Grass and CARDAMOM to produce landscape analyses of grassland C cycling under varied management systems using earth observation.

2. Materials and methods

2.1. DALEC-Grass

DALEC-Grass is a development of the DALEC model in which a number of processes related to grass growing, cutting and grazing have been introduced (Smallman et al., 2017). The model is written in fortran and its code is available online at https://github.com/GCEL/DALEC-Grass. DALEC-Grass is a parsimonious terrestrial ecosystem C cycling model of intermediate complexity which tracks the dynamics of three plant C pools and two dead organic matter pools. DALEC-Grass does not resolve explicitly mixtures of grasses and biodiversity, and water and nitrogen (N) cycling are not described. The model is driven by temperature, short-wave radiation, vapour pressure deficit and CO_2 concentration (Table 1). Carbon enters the ecosystem via gross primary production (GPP) which is partitioned into autotrophic respiration or allocated to various plant pools (Fig. 1). The model simulates the turnover of plant C pools to litter and soil organic matter based on both mortality and grazing/cutting. The mineralisation (i.e. heterotrophic respiration) and decomposition of litter and soil organic C pools are temperature dependent first order processes.

DALEC-Grass has 25 parameters impacting photosynthesis, litter production and decomposition, fractional allocation of C, and climate sensitivity of phenology and decomposition. A further 8 parameters relate to initial conditions of C pools and to management impacts of grazing and cutting (see Table 5 in supplementary material). The calculations in DALEC-Grass are performed on a daily basis by default. A component of DALEC-Grass is the Aggregated Canopy Model (ACMv1); a photosynthesis model that emulates a detailed mechanistic model, and that uses daily meteorological data to estimate GPP (Williams et al., 1997). The duration and intensity of the grass growing period is calculated following the growing season index (GSI)

approach (Jolly et al., 2005). The GSI method uses information on vapour pressure deficit (VPD), daylength and daily minimum temperature to adjust the plant's physiological progress (Smallman et al., 2017).

The net primary productivity (NPP) C, which remains after accounting for C losses via autotrophic respiration, is allocated to root, stem and leaf tissues. In DALEC-Grass, the above- to below-ground C allocation balance is dynamic and is calculated on a daily basis using the architecture-dependent strategy presented in Reyes et al. (2017). According to this approach, the C that is transferred to the fine root C pool is linked to above-ground biomass and increases after the plant has grown a sufficient quantity of leaves. This linkage is achieved by the following equation :

$$F_{root_t} = 1 - exp(-1 * P4 * LAI_t) \tag{1}$$

where F_{root_t} is the fraction of NPP C that goes to the root C pool on day t, LAI_t is the LAI of the sward on day t and $P4$ is a model parameter. The remaining NPP C is allocated to above-ground biomass. Its partitioning to the stem and leaves C pools is based on the idea that increasing stem mass is needed to support increasing leaf mass but the stem to leaf ratio is dynamic and not constant. The C allocation to leaves and stems is calculated using parameter $P29$ within the following equations :

$$F_{leaf_t} = NPP_t * (1 - (P29 * (LAI_t / LAI_{max}))) \tag{2}$$

$$F_{stem_t} = NPP_t * (P29 * (LAI_t / LAI_{max})) \tag{3}$$

where F_{leaf_t} is the fraction of NPP allocated to the leaf C pool on day t, F_{stem_t} is the fraction of NPP allocated to the stem C pool on day t, LAI_t is the LAI of the sward on day t and LAI_{max} (set to 6 m^2 m^{-2}) is a maximum LAI for managed grasslands.

Animal grazing and grass cutting is imposed as a time series forcing. The number of livestock units (LSU) per ha per day determines the animal grazing intensity. The amount of C that one LSU removes from the grassland via grazing is estimated by multiplying the LSU value by a "dry matter demand per weight of 1 LSU" parameter (P31); with the standard weight of one LSU being equal to 650kg. The resulting dry matter (DM) value (in kgDMha^{-1}) is converted to gCm^{-2} and removed from the C pool of the foliage. DALEC-Grass has a set of internal mechanisms through which it

can accept/perform or reject/skip a grazing instance. These mechanisms reflect the logical assumption that there is a minimum amount of above-ground biomass that has to remain after grazing for grass to be able to grow the following days; i.e. grazing is not simulated when the simulated above-ground biomass is below a threshold. This minimum biomass threshold is a model parameter (P27) and a similar parameter and concept is applied for cutting (P28); i.e. cutting cannot take place when the simulated above-ground biomass is below a threshold. These mechanisms exist to ensure there are no unrealistic combinations of livestock density and simulated grass biomass.

DALEC-Grass uses a simple scheme to convert the amount of C in grass into (1) C in animal-respired CO_2; (2) C in methane (CH_4) produced via digestion; and (3) C in animal excrement. Of the total amount of C ($gCm^{-2}d^{-1}$) that is grazed : (1) 54% is lost to the atmosphere as CO_2; (2) 4% is lost to the atmosphere as CH_4; (3) 32% returns to the soil as C in excrement; and (4) the remaining 10% stays in the animal's body. In reality the conversion factors of grazed C are dynamic, they depend on animal type, weight and age and vary even between animals that have the same aforementioned characteristics (Vertès et al., 2018; Snow et al., 2014). The grazed C conversion factors used in DALEC-Grass are generic in order to reflect different estimates for beef/dairy cattle and sheep and were extracted from the relevant literature (Bell et al., 2016; Lee et al., 2017; Worrall and Clay, 2012; Parsons et al., 2009). In terms of modelling soil C dynamics, DALEC-Grass uses a simple soil C scheme, in which plant residue and excrement-contained C go into a single litter pool. Litter C undergoes temperature-dependent decomposition with part of the C lost as heterotrophic respiration while the remainder is moved into a single slowly-decomposing soil C pool that represents the soil's organic matter.

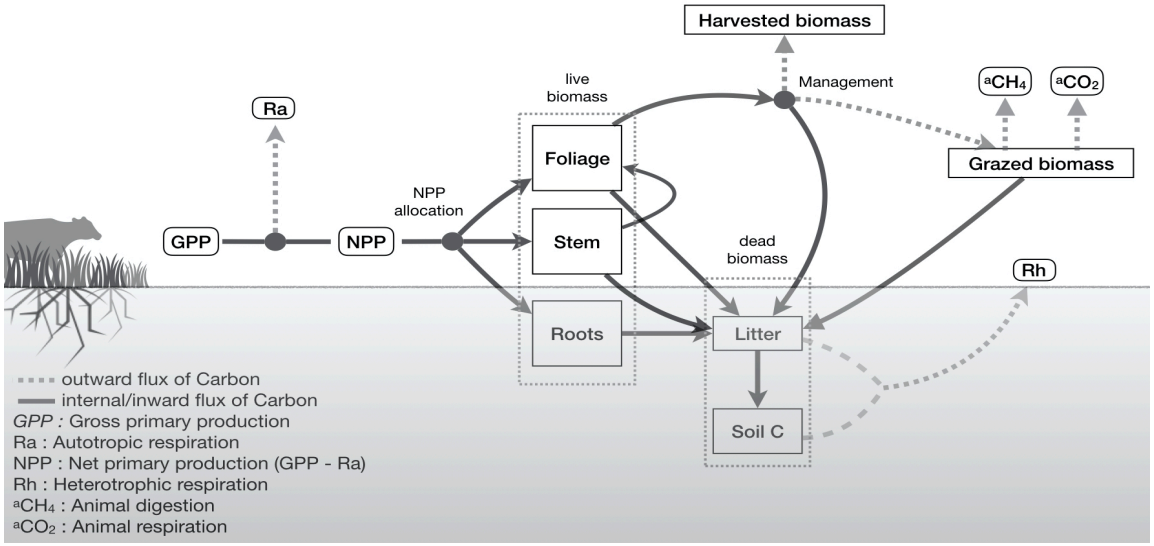

Figure 1: Diagram of the DALEC-Grass model. Daily GPP is calculated by the ACM model. DALEC has 5 pools: leaves, stem, roots, litter and soil organic matter.

Table 1: DALEC meteorological and management inputs

Variable	**units**
Minimum daily temperature	^{o}C
Maximum daily temperature	^{o}C
Short-wave radiation	MJm^{-2}day
Atmospheric CO_2 concentration	ppm
21-day average minimum temperature	C
21-day average photoperiod	sec
21-day average vapour pressure deficit	Pa
Animal density	livestock units per ha

2.2. Carbon Data Model Framework

DALEC-Grass is integrated into the Carbon Data Model Framework (CARDAMOM) (Bloom et al., 2016). CARDAMOM is a MDF framework that uses Bayesian inference to approximate the joint distribution of model parameters. This approximation is done using a function of the likelihood of each sampled parameter vector. The Bayes' theorem forms the basis Bayesian inference:

$$P(\theta|D) = \frac{P(D|\theta)P(\theta)}{P(D)} \tag{4}$$

where θ represents the parameters, D the observed data, $P(\theta|D)$ the posterior distribution of parameters, $P(D|\theta)$ the likelihood of θ given D, $P(\theta)$ the prior distribution of parameters and $P(D)$ the marginal distribution of D (normalisation constant). The effectiveness of Bayesian inference stems from the fact that the posterior distribution of parameters is proportional to the likelihood:

$$P(\theta|D) \propto P(D|\theta)P(\theta) \tag{5}$$

Markov Chain Monte Carlo (MCMC) is a group of algorithms that are used to sample from probability distributions (Chib and Greenberg, 1995). For a discussion on MCMC theory we refer to van Ravenzwaaij et al. 2018 and for a description of different MCMC algorithms we refer to Houska et al. 2015. In our implementation of CARDAMOM, the Metropolis-Hastings (MH) MCMC algorithm is used. Metropolis-Hastings creates a Markov chain

by deciding whether each sampled θ is accepted or rejected after comparing its likelihood to that of the last accepted θ. This comparison is done using the acceptance ratio (A) :

$$A = \frac{f(\theta')}{f(\theta)} \tag{6}$$

where θ' is the sampled θ under examination and f is a function proportional to $P(\theta|D)$. For this study, MH used a metric that describes the model's predictive skill against observed variables as a surrogate likelihood. This metric is named *accuracy* and is described in Myrgiotis et al. (2016). Accuracy quantifies the number of simulated data points that fall within the respective measured range (i.e. standard deviation assuming normal distribution for D) while it also considers possible time lags between measured and simulated time series. Accuracy can take any value between 0 (no simulated points within the observed range) and 1 (all simulated points within the observed range). The consideration of time lags when calculating the metric allows CARDAMOM to capture some of the impacts that possible temporal uncertainties in model inputs can have on model outputs (Myrgiotis et al., 2018). Similarly, delayed responses of the grassland's physiology and/or biogeochemistry to driving variables, which could appear due to model formulation uncertainty and/or parametric uncertainty, can also be captured. Moreover, the model's internal mechanisms can lead to instances when e.g. a day's grazing, even though it is specified in the inputs, is not modelled because there is not sufficient simulated grass biomass on that day. This can lead to time lags in LAI fluctuation and affect the level of fit between modelled and measured data.

For each assimilated variable (LAI and NEE) we provide an estimate of uncertainty around the measured data points. For LAI the uncertainty is set equal to $\pm 15\%$ of the mean measured value (Van Wijk and Williams, 2005). Attributing uncertainty levels around measured NEE data is more complicated because most measured datasets depend on a single flux tower and do not provide uncertainty estimates. In this study the uncertainty around the measured NEE data is set equal to ± 1 gCm^{-2} (Hill et al., 2012; Revill et al., 2016). The overall setup of the implementation of MH in CARDAMOM is the following :

- 10 chains are run in parallel

- Each chain has 100 million steps
- The initial 10% of all accepted steps is used as burn-in
- At each step of the Markov chain the MH algorithm:
    1. obtains a sampled parameter vector
    2. calculates the objective function (i.e. accuracy metric)
    3. calculates A and :
        - If $A > 1$ then θ' is accepted
        - If $A >$ a uniform random number [0.3 - 1] then θ' is accepted
        - If $A <$ a uniform random number [0.3 - 1] then θ' is rejected

A list of ecological and dynamic constraints (EDCs) is used in CARDAMOM to refine the parameter space that the MH sampling explores (Bloom et al., 2016). EDCs are checks of the mathematical, ecological and biogeochemical sanity of the sampled model parameter combinations and model outputs (pools, fluxes). These checks are performed in CARDAMOM before and/or after each run of DALEC-Grass, which is performed to estimate the likelihood of each sampled parameter vector in MH. Altogether, EDCs reflect existing knowledge on grassland ecosystem functioning. Table 2 outlines the EDCs that were used with CARDAMOM in this study. Ecological and dynamic constrains are a key feature of the CARDAMOM MDF framework. Retrieving posterior parameter distributions that are mathematically and theoretically sound depends on the use of appropriate EDCs. In this regard, the present study is a test of CARDAMOM's grassland-specific EDCs.

The assessment of if and when a MCMC algorithm has converged to the stationary distribution of parameters is an essential part of its implementation. The difficulty of convergence assessment increases with the number of parameters and no single convergence diagnostic is generally accepted as being suitable for every application (Brooks and Gelman, 1998). When multiple chains are explored, such as in CARDAMOM, convergence diagnostics based on the comparison of inter and intra-chain variances are appropriate. The Gelman-Rubin (GR, see supplementary material) is one of the most widely used convergence diagnostics of this type and was used to assess chain convergence in this study (Gelman and Rubin, 1992). The equations used for calculating the potential scale reduction factor (PSRF) of the GR method

and the results of chain convergence assessment are presented in the supplementary material.

2.3. Field measured data

Measured data from two managed grassland sites, of contrasting soil and climatic conditions, in eastern (Easter Bush) and southern (Crichton) Scotland are used in this study.

2.3.1. Easter Bush

Easter Bush is located in South East Scotland, 10 km south of Edinburgh (03°02'W, 55°52'N, 190 m above sea level). The mean annual rainfall between 2002 and 2010 was 947 ±234 mm and the mean annual temperature was 9.0 ±0.4 °C. The field has been under permanent grassland management for more than 20 years with a species composition of >99% perennial ryegrass (*Lolium perenne*) and < 0.5% clover (*Trifolium repens*). The soil type is an imperfectly drained Eutric Cambisol (FAO classification) with a pH of 5.1 (in H_2O), a clay fraction of 20-26% (Clayey Loam to Sandy Loam) and a soil organic carbon content of 4% (0-10 cm depth). The grassland was grazed continuously by heifers in calf, ewes and lambs at different stocking densities. The grass was cut for silage in June and August 2002 and in May 2003. Ammonium nitrate fertiliser was applied to the field 3-4 times per year, usually between March and July at an average of 56 kg N ha^{-1} per application. An additional fifth mineral N application was applied as urea in 2008 and organic manure was applied in September 2004 and March 2005 as cattle slurry. Vegetation for above ground biomass and LAI measurements were collected from 4 to 6 quadrats (0.0625 m^2) per sampling occasion. The leaf area was analysed using a Li3100 Area meter (LI-COR inc. Lincoln, Nebraska, USA). Fresh weight of biomass samples were recorded before samples were dried at 80^{o}C for 24 hours and dry weight was measured. NEE was measured by an eddy covariance system consisting of a fast response 3D ultrasonic anemometer (Metek USA-1, Metek GmbH, Elsmhorn, Germany) and a fast closed path CO_2-H2O analyser (LI-COR 7000 infra-red gas analyzer, LI-COR, Lincoln, NE, USA). Quality control of the eddy covariance data followed the procsedure proposed by Foken and Wichura (1996). Missing NEE data were gap-filled using the online tool developed by Reichstein et al. (2005). Soil respiration rates were measured weekly (297 times between 2003 and 2010) at 4 locations using a closed dynamic chamber (volume 1334 cm^3, cover area 78.5 cm^2, PP-Systems, Hitchin, UK), which was

Table 2: Ecological and Dynamic Constraints

Index	**Description**
1	Fluxes cannot be negative
2	Pools cannot be negative
3	GSI-related minimum parameters cannot be larger than maximum parameters
4	Turnover rate of soil organic matter cannot be larger than that of litter
5	Initial SOM pool cannot be smaller than the sum of all other pools
6	Annual GPP cannot be more than 2000 g C m^{-2} (Xia et al., 2017; Gilmanov et al., 2007)
7	Annual GPP cannot be less than 500 g C m^{-2} (Xia et al., 2017; Gilmanov et al., 2007)
8	Daily GPP cannot be more than 20 g C m^{-2} (Xia et al., 2017; Gilmanov et al., 2007)
9	Annual ecosystem respiration cannot be more than 2000 g C m^{-2} (Xia et al., 2017; Gilmanov et al., 2007)
10	Annual ecosystem respiration cannot be less than 500 g C m^{-2} (Xia et al., 2017; Gilmanov et al., 2007)
11	Daily ecosystem respiration cannot be more than 15 g C m^{-2} (Xia et al., 2017; Gilmanov et al., 2007)
12	LAI cannot exceed 6 m^2 m^{-2}
13	Minimum daily estimated root to shoot ratio cannot be less than 1 (Mokany et al., 2006)
14	Daily cut grass biomass cannot be more than 300 g C m^{-2} or less than 50 g C m^{-2} (Qi et al., 2017)

placed onto soil and vegetation. The CO_2 increase within the chamber was monitored over 30-180 s by a portable sensitive infrared gas analyser (EGM 2, PP-Systems). It should be noted that the area covered for the soil respiration measurements also included vegetation and, therefore, measurements are effectively equivalent to ecosystem respiration (the sum of autotrophic and heterotrophic respiration). The data were converted from μmol CO_2 m^{-1} s^{-1} to g CO_2-C m^{-2} d^{-1} using the daily minimum and maximum temperatures and a Q10 equal to 2 (Meyer et al., 2018; Barba et al., 2018).

2.3.2. Crichton

The field experiment was located at Crichton Royal Farm, Dumfries (55° 2'3"N, 35° 35'1" W) in South-West Scotland, on a long-term permanent grassland site (6.53 ha) used for intensive dairy production (Bell et al., 2016). The landscape was open grassland dominated (proportion of total harvested biomass $>$ 99%) by perennial ryegrass (*Lolium perenne*) with white clover (*Trifolium repens*), creeping buttercup (*Ranunculus repens*) and chickweed (*Stellaria media*) being minor sward constituents. The Crichton site is representative of a wet climate zone, with a 30 year (1971-2000) long-term average rainfall of 1140 mm, and mean annual temperature of 9.3 ^{o}C. The soil was a Eutric Cambisol (FAO classification) and had a free-draining sandy to sandy-loam light texture. The soil organic C concentration (0-10 cm) was 5.25% (4.3-6.2%), and the pH varied between 5-6.3 at this site. The long term management of the site involved a rotation between cutting (with three cuts per year) and summer grazing. Between March and July 2015, 226 kg N ha^{-1} were applied as slurry (4 applications) and synthetic fertiliser (2 applications). A sampling grid (20m * 20m) was marked out in the field at the beginning of the measurement campaign in June 2015. Leaf area index (LAI), aboveground biomass and respiration at soil surface (Rs) were made on four occasions, and root biomass on two occasions during June and July 2015. LAI was measured using a LAI-2200C Plant Canopy Analyzer (Licor Biosciences, Lincoln NE) at each point of the sampling grid. Aboveground biomass was measured using a rising plate meter calibrated against destructive biomass sampling. Root biomass was destructively sampled by taking replicate 2 cm diameter soil cores and dividing into 0-10 and 10-20 cm depths from positions adjacent to the collars used for Rs measurements. Soil respiration (Rs) was measured,at midday, on four dates, using a potable PP Systems Infra-red EGM4 Gas Analyser linked to a SRC-1 soil respiration chamber. The chamber (10 cm of diameter and 15 cm height) was equipped

with a fan, and was inserted into bare soil with a basal cutting ring to a depth of 2 cm during measurements. The air from the chamber was send to the analyser at flow rate of 0.2 l min^{-1}. After the chamber equilibrated the CO_2 concentration was measured every 5 seconds and the flux was calculated from the concentration increase over approximately 60 seconds time using a linear regression. Net ecosystem exchange of CO_2 was measured using an eddy covariance tower (EC) sited within the field (11 m height), with a Gill R3 sonic anemometer (Gill Instruments, Lymington UK) and a Licor LI700 CO_2 analyser (Licor Biosciences, Lincoln NE). Velocity measurements were rotated to minimize the mean vertical velocity. A site specific cospectral model was developed, based on sensible heat fluxes. Similarly, sensor specific models of sensor frequency response attenuation were developed and combined with the cospectral models to determine, and then apply, frequency response corrections. The resulting fluxes were screened for plausibility instrument diagnostics and for individual deviations from the group mean by more than two standard deviations.

2.4. Methodology

The volume of field-measured data and the range of measured variables at Easter Bush and Crichton allows us to test DALEC-Grass and CARDAMOM in detail. In designing the methodology of the study we considered two main aspects: (1) the efficient use of the available field-measured data and (2) the ability to relate our computational experiments with the envisioned application of DALEC-Grass in MDF studies. For these reasons, the use of LAI observations has a particular importance. LAI is a physiology-related variable, for which data can be collected rather easily and frequently at the different spatial scales that DALEC-Grass can be applied i.e. farm, landscape, region. This contrasts with what is the case for the other measured variables examined in this study with the possible exception of aboveground biomass for which satellite data are increasingly available. Because of the lack of accurate satellite-based LAI data for Easter Bush during the simulated period, field-measured LAI data were used in this study.

Initially, all DALEC-Grass parameters have a uniform distribution i.e. only a realistic minimum and maximum value is known for each of them. In order to refine these uniform distributions we drive DALEC-Grass with 3 years of climate and management data for the Easter Bush site while assimilating in-situ NEE and LAI observations (step 1). Through this parameter

calibration step we expect parameter distributions to become more representative of managed (cut and grazed) grasslands. It should be clarified that the term calibration is used to refer to the refinement of the prior distribution of parameters and not the parameters themselves. During calibration, the calculated accuracy metric is the mean of the accuracy for LAI and the accuracy for NEE. In order to test the MDF framework we, then, run DALEC-Grass (step 2) for 6 additional years at Easter Bush, this time assimilating only the available LAI observations. We assess the model's performance at Easter Bush by comparing model outputs with independent in-situ data on NEE (flux tower based) and ecosystem respiration (ER, chamber based). Moreover, we run DALEC-Grass with one year of climate and management data from Crichton while assimilating the available field-measured LAI data (step 3). The model's performance at Crichton is assessed by comparing model outputs with independent in-situ data on NEE, above and below-ground biomass and soil respiration. The four steps of our computational experiment are :

1. Calibration of DALEC-Grass parameters: Implementation of CARDAMOM at Easter Bush by assimilating 3 years (2002-2004) of LAI and NEE observations.

2. MDF at Easter Bush: Using the calibrated distributions (step 1), implementation of CARDAMOM at Easter Bush for 6 years (2005-2010) by assimilating the corresponding LAI observations.

3. MDF at Crichton: Using the calibrated distributions (step 1), implementation of CARDAMOM at Crichton for 2015 by assimilating LAI observations.

4. Quantitative assessment of MDF at steps 1,2 and 3 against the assimilated data and against independent data.

In order to assess model accuracy and precision we calculate, for each variable examined, the percentage of observed data points (i.e. mean of observations) that fell within the 95% confidence intervals (CI) produced by the model runs. We refer to this metric as *overlap* and present it as a percentage that can take a value between 0 and 100. We also calculate (1) the Root Mean Squared Error (RMSE) to quantify the difference between measured and modelled data; (2) the bias in model predictions; and (3) the Pearson correlation coefficient (r) to quantify how well the trends in measured

data are captured by the model (for equations see Myrgiotis et al. (2016)). It should be noted that –where mentioned– estimates of the uncertainty of measurements come from using the RMSE equation after replacing base of the exponent with the sum of 2 standard deviations of each measured data point.

3. Results

3.1. Easter Bush

Three years (2002-2004) of measured LAI and NEE data were assimilated by CARDAMOM to calibrate the distributions of DALEC-Grass parameters. For the calibration period, 25 % of LAI observations and 90 % of NEE observations fell within the 95 % confidence interval of the CARDAMOM analysis while r was 0.25 and 0.56 respectively (Table 3). The calibrated parameter distributions were used to run DALEC-Grass for the subsequent 6 years of measurements (2005-2011); this time assimilating available measured LAI data only.

For the 2005 to 2011 MDF period, 85% of the measured weekly-mean NEE and 82% of the daily LAI data points lied within the 95% CIs. The variation in NEE ($r = 0.70$) and LAI ($r = 0.74$) was well captured. DALEC-Grass tended to overestimate both NEE (bias=0.38 gCm^{-2}) and LAI (bias = 0.47 m^2m^{-2}). We used a 15% relative uncertainty around the measured LAI data during the MDF process with CARDAMOM. We found that the RMSE of the measured against modelled LAI data was 10% lower than the mean uncertainty of the measured LAI data. We repeated this process for NEE, and found that the estimated RMSE was equal to the uncertainty attributed to the measured data during the MDF process (i.e. 1 gCm^{-2}) .

DALEC-Grass was able to capture the patterns and magnitudes in measured ER (Fig. 4). The comparison of modelled and measured ER estimates produced a r of 0.79, which reflects the model's skill in representing ER patterns. In terms of the relative size of ER, 83% of the mean measured ER data were within the modelled 95% CI. The estimated RMSE (1.5 gCm^{-2}) was smaller than the average uncertainty of the measured data (1.65 gCm^{-2}) (Table 3). The inter-annual patterns in MDF-estimated NEE, ER and GPP mirror the measured data as presented in Jones et al. 2017 (Fig. 5).

The mean simulated harvest (283 $gCm^{-2}a^{-1}$) was just 3% higher than the measured harvest (270 $gCm^{-2}a^{-1}$) in 2002 and 30% lower than the 2003 measured harvest (170 $gCm^{-2}a^{-1}$) (Jones et al., 2017). However, both in

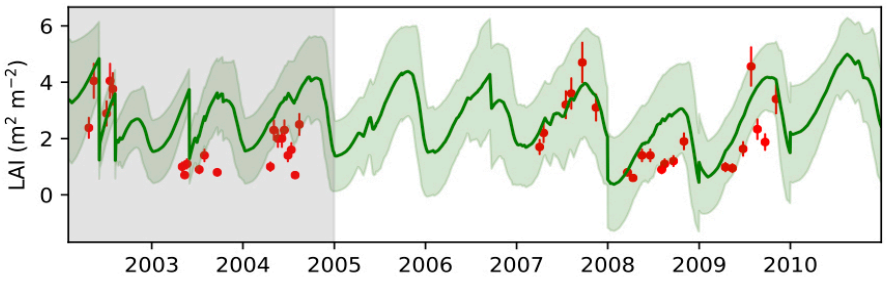

Figure 2: Modelled and measured daily Leaf Area Index (LAI) at the Easter Bush site. Grey-shaded area (2002-2004) shows the parameter calibration period. The unshaded area (2005-2011) represents the LAI data assimilation period. The mean modelled LAI and the CARDAMOM-estimated 95% confidence intervals presented in green. The measured LAI and its 15% relative uncertainty presented in red.

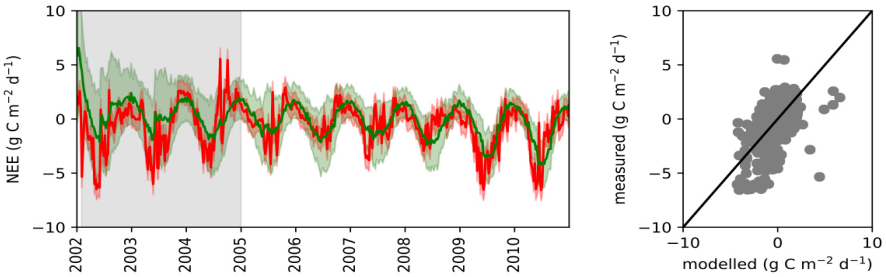

Figure 3: Weekly mean Net Ecosystem Exchange (NEE) at the Easter Bush site. From left to right: (1) Time series of measured (red) and modelled (green) weekly mean NEE. The green-shaded area represents the 95% confidence intervals and the red-shaded area represents the uncertainty around the measured NEE (1gCm^{-2}d^{-1}). The parameter calibration period (2002-2004) is shown as grey-shaded area. (2) Scatter plot of measured and corresponding modelled weekly mean NEE.

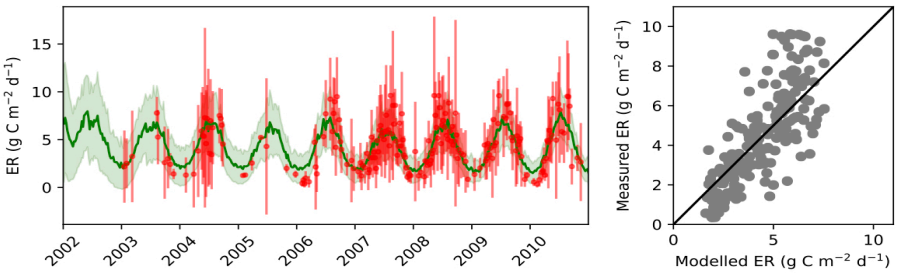

Figure 4: Weekly mean Ecosystem Respiration (ER) at the Easter Bush site. From left to right: (1) Time series of measured (red) and modelled (green) weekly mean ER. The green-shaded area represents the 95% confidence intervals and the red error bars the uncertainty around the measured ER. (2) Scatter plot of measured and corresponding modelled weekly mean ER.

Table 3: Model performance metrics for Easter Bush

Variable	**Time period**	**r**	**Bias**	**Overlap**	**RMSE**
LAI	2002-2004	0.34	1.33	25 %	1.6
	2005-2010	0.74	0.47	82 %	1.0
NEE	2002-2004	0.56	0.95	90 %	2.11
	2005-2010	0.70	0.38	85 %	1.00
ER	2002-2010	0.79	-0.07	83 %	1.5

Weekly mean data used for Net Ecosystem Exchange (NEE) and ecosystem Respiration (ER). Overlap shows the percentage of observed data that lie within the model-based 95% CIs. Bias and RMSE in gCm^{-2} for ER and NEE and in m^2m^{-2} for LAI.

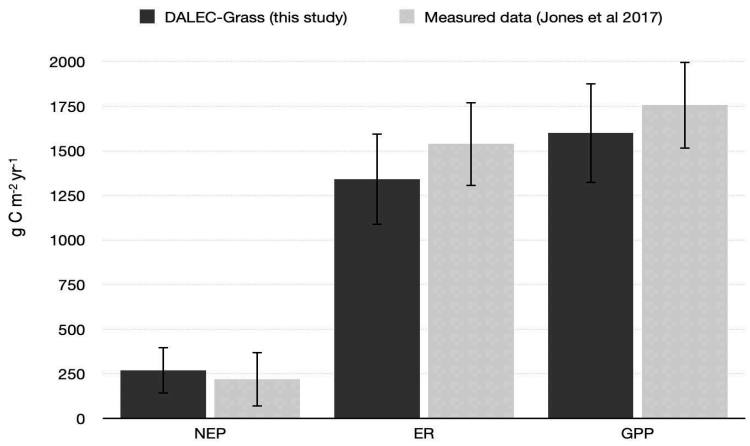

Figure 5: Comparison of MDF-based and measurements-based (after Jones et al. 2017) annual Net Ecosystem Production (NEP), Gross Primary Productivity (GPP) and Ecosystem Respiration (ER). Bars show the mean $gCm^{-2}yr^{-1}$ between 2002 and 2010 and error bars show the inter-annual standard deviation.

2002 and 2003 the measured annual harvest was within the CARDAMOM estimated 95% CIs. The simulated Easter Bush grassland behaved as a typical UK permanent grassland producing an average of 262 gCm^{-2} (5.6 $tDMha^{-1}$) of grass biomass per year. This level of biomass availability and removal is within the expected range (353 $\pm$96 $gCm^{-2}a^{-1}$) as estimated in a recent study by Qi et al., 2017. Finally, DALEC-Grass estimated a mean annual input to soils of 710 $gCm^{-2}a^{-1}$ in the form of root and leaf litter.

3.2. Crichton

The calibrated parameter distributions retrieved for Easter Bush (2002-2004) were used as priors for the CARDAMOM analysis at the Crichton site. Four field-measured LAI data points were available for assimilation (Fig. 6). The assimilation of measured LAI data also affected the fit between measured and modelled aboveground biomass and grass harvest. All four measured LAI data points were within the modelled 95% CIs. However, the model did not capture the first of four aboveground biomass measurements. It should be noted that neither the quantity of grass harvested nor the amount of aboveground biomass (at any point in time) were provided to the model during the LAI data assimilation in CARDAMOM. Despite this discrepancy, the two simulated harvests removed 276 gCm^{-2} (5.8 $tDMha^{-1}$) from the

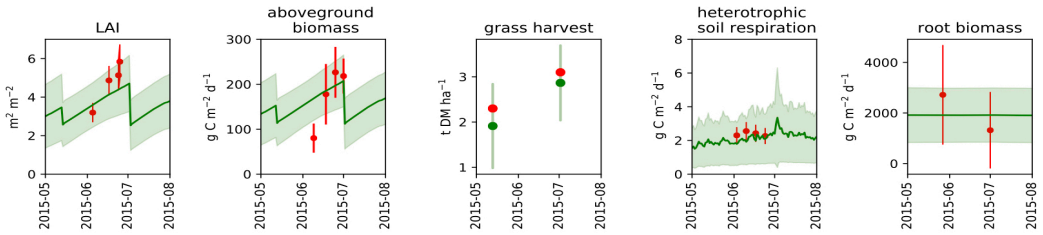

Figure 6: Modelled (green) and measured (red) LAI, aboveground biomass, grass harvest, root biomass and heterotrophic respiration at the Crichton site. The red error bars represent the uncertainty around the measured data.The CARDAMOM-estimated 95% confidence intervals are presented in green shading

grassland, and each measured harvest yield was within the corresponding CARDAMOM's 95 % CI (Fig. 6).

DALEC-Grass was successful in reproducing the measured patterns and magnitudes of NEE. The estimated correlation coefficient was 0.88, the mean bias was 0.25 gCm^{-2}, the RMSE was 0.96 gCm^{-2} and all the of the measured data were within the 95% CIs (Fig. 7). Notwithstanding the large variability among the collected samples of root biomass, the mean simulated amount of C contained in grass roots was within the respective measured ranges (Fig. 6). DALEC-Grass currently does not separate autotrophic respiration C into above and belowground fluxes. In order to allow for a comparison between measured and simulated respiration data we assumed that between 40% and 60% of total surface respiration can be attributed to heterotrophic sources (Li et al., 2018). While not directly measured we, henceforth, refer to heterotrophic respiration data as measured data. The comparison between measured and modelled heterotrophic respiration showed that all four measured data points lied within the 95% CI (Fig. 6). Finally, DALEC-Grass estimated that 780 $gCm^{-2}y^{-1}$ were added to Crichton's soil in 2015 in the form of root and leaf litter.

3.3. MDF-retrieved distributions

Model parameter distributions were calibrated using 3 years of LAI and NEE data from Easter Bush (calibration period). This calibration process led to reductions in the length of the uniform prior distributions that varied according to parameter. The average prior length reduction was 47% with achieved reductions being between 3% and 99%. Details on the application of CARDAMOM for parameter distribution calibration include pos-

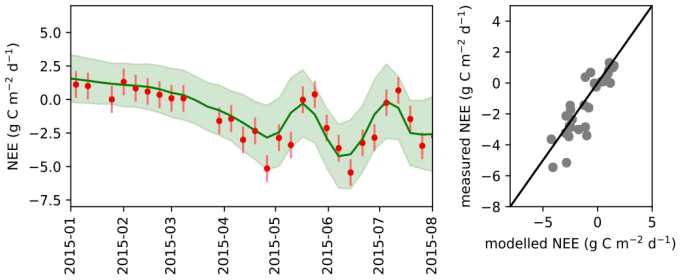

Figure 7: Weekly average Net Ecosystem Exchange (NEE) at Crichton. From left to right: (1) Time series of measured (red) and modelled (green) weekly mean NEE. The green-shaded area represents the 95% confidence intervals and the red error bars represent the uncertainty around the measured NEE (1gCm^{-2}d^{-1}). (2) Scatter plot of measured and corresponding modelled weekly mean NEE.

Table 4: Model performance metrics for Crichton

Variable	**r**	**Bias**	**Overlap**	**RMSE**
NEE (weekly mean)	0.88	0.25	100 %	0.96

Weekly mean data used for Net Ecosystem Exchange (NEE). Overlap shows the percentage of observed data that lie within the model-based 95% CIs. Bias and RMSE in gCm^{-2}.

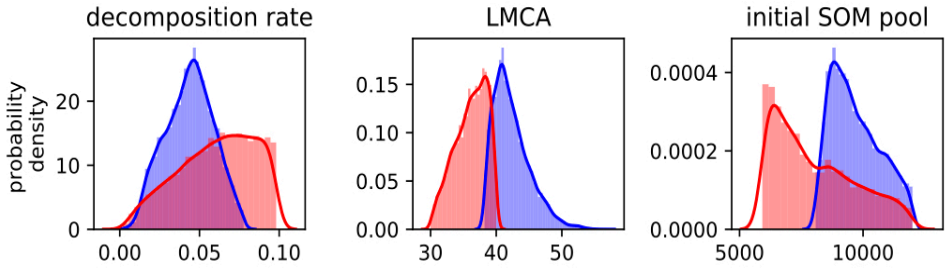

Figure 8: Probability densities of the posterior distributions for three selected DALEC-Grass parameters based on MDF results at Easter Bush (in red) and Crichton (in blue).

terior means, maximum-a-posteriori-probability and prior length reduction, and are presented in Table 5 in supplementary material along with information on MCMC chain convergence assessment (Fig. 9).

4. Discussion

The results of this study show how MDF can quantify C dynamics in grasslands under variable grazing and cutting regimes. A limited number of in-situ LAI observations were assimilated through the CARDAMOM MDF framework in order to test the predictive skill of DALEC-Grass against 7 years of data at two Scottish grasslands. At the grazed Easter Bush grassland 21 in-situ LAI observations were assimilated to produce time series of C fluxes (NEE and ER) that closely matched corresponding measurements (eddy covariance and chamber-based fluxes, respectively). At the harvested Crichton site 4 in-situ LAI observations were assimilated and CARDAMOM produced robust estimates of above and below-ground biomass C pools and NEE C fluxes. The use of CARDAMOM also allowed us to handle observational and model parametric uncertainty and provide a level of predictive uncertainty for the examined variables.

4.1. Model performance

Our MDF approach provides a probabilistic solution to the parameter identification problem. Among the factors that affect the robustness of model analyses are how measurement uncertainty and model parameter identification are assessed. In this study, measured data uncertainty has been considered at the parameter retrieval stage, through the use of the accuracy metric as the cost function, and at the model evaluation stage, through the use of the CIs in quantifying and expressing model prediction skill. As a consequence, the results of simulations are distributions of parameter values and provide a quantitative analysis of the parameter-induced uncertainty around the model's results. The average uncertainty around predicted C fluxes (NEE, ER) was less-than-or-equal to that attributed to NEE (1 $gCm^{-2}d^{-1}$ based on literature) and estimated from ER measurements (1.65 $gCm^{-2}d^{-1}$) (Hill et al., 2012; Revill et al., 2016).

CARDAMOM's key novelty is the use of ecological and dynamical constraints (EDCs) as conditions imposed on the parameter retrieval process. The aim of including EDCs is to ensure that the MDF process respects a set of mathematical, ecological and biogeochemical rules. In practice, the

success of the MDF process can be judged by the level of fit between the outputs of DALEC-Grass and the assimilated measured data. However, in this study, we wanted to have a stricter assessment of DALEC-Grass and CARDAMOM. We used 3 years of measured data on LAI and NEE (Easter Bush) to calibrate the parameter distributions and, thereafter, used the refined prior distributions and LAI data assimilation for the remaining 6 years of data in Easter Bush and the one year of data in Crichton. The evaluation of MDF performance against NEE (Easter Bush and Crichton), ER (Easter Bush), biomass (Crichton) and heterotrophic respiration (Crichton) showed that DALEC-Grass was able to describe the examined C dynamics in managed grasslands with good accuracy. The mean overlap for NEE, ER and LAI during the MDF implementation was equal to 88% and RMSE was less than, or equal to, the respective measurement uncertainty (for NEE and ER). We argue that calculating the overlap along with the RMSE is an effective way to express the level of agreement between modelled and measured data for which uncertainty is quantified.

4.2. Retrieved parameter distributions

The MDF application at Easter Bush and Crichton adjusted the distributions of model parameters to fit the observed LAI at each site. CARDAMOM was able to retrieve parameter distributions that led to model outputs that fit with the available observations while being conceptually and mathematically sound, as proven by the stability of the CIs for all the variables examined in the two grasslands. The parameter distributions obtained for each grassland did not differ for most parameters. However, for three parameters CARDAMOM produced informatively different distributions at the two grasslands (Fig. 8). For the "litter decomposition rate" parameter, the addition of animal excrement C to the soil's litter C pool led CARDAMOM to retrieve a higher decomposition rate (i.e. more litter C goes into the SOC pool) in Easter Bush compared to Crichton, where there was no grazing during the measurement period. A higher leaf C per area (LMCA) was retrieved for Crichton compared to Easter Bush. This result suggests that the vegetation of cut Crichton grassland is more C dense than that of the grazed Easter Bush grassland, something that relevant studies confirm (Liu et al., 2017; Zheng et al., 2015; Laliberté et al., 2012). We argue that the ability to infer the relative difference in vegetation C density between grasslands is an important outcome produced by the combination of the model's management related processes and the CARDAMOM EDCs. Moreover, DALEC-Grass depends

on a simple soil C scheme and CARDAMOM is given a wide prior range for initial SOC pool size parameter. Despite this, CARDAMOM suggests that, considering productivity levels, allocation patterns and EDCs, Easter Bush had a lower soil C content than Crichton. These results are confirmed by field-measured data, which show that SOC in Easter Bush is around 30% less than SOC in Crichton (COSMOS-UK, 2019).

Based on the DALEC-Grass simulations and the corresponding measured data Easter Bush and Crichton were net sinks of C during the simulated periods. Both grasslands had a simulated annual aboveground biomass productivity that is within the observed limits (i.e. 238-429 $gCm^{-2}yr^{-1}$). The parsimonious mechanisms used in DALEC-Grass to describe grazing and cutting were effective and the retrieved parameter distributions for the relevant parameters are in agreement with relevant observations (Genever and Buckingham, 2016). For Easter Bush, CARDAMOM inferred from the data and modelling that grazing occurs when the total aboveground biomass is $>$ 38-47 gCm^{-2} (0.8-1.0 $tDMha^{-1}$). The distribution of the minimum pre-cutting aboveground biomass for Easter Bush showed that $\approx$120 gCm^{-2} (2.8 $tDMha^{-1}$) is the most likely value for this parameter. The minimum pre-cutting and pre-grazing aboveground biomass parameters (P27 and P28) also define how much biomass will be left standing immediately after each cutting and their posterior distributions suggest a minimum harvest of 86 gCm^{-2} (1.8 $tDMha^{-1}$). This is a realistic, albeit low, minimum harvest yield for the UK where grasslands can be cut up to three times per year Qi et al., 2017. Finally, DALEC-Grass results showed that the annual amount of C added to the soil as root and leaf litter is $\approx$ 10% more in Crichton compared to that estimated for Easter Bush. This difference is a result of the adaptation of C allocation patterns in response to the presence of grazing animals which also leads to a lower leaf C content in the grazed ecosystem (Easter Bush) (Hao and He, 2019; Chen et al., 2015; Mcsherry and Ritchie, 2013).

4.3. Limitations

Our analysis highlights areas for potential improvement in both the model and the MDF framework. DALEC-Grass is frugal with its number of parameters and therefore the processes it incorporates. The results of this study showed that there is still a margin for improvement, which can be inferred from the different evaluation metrics. Moreover, the model requires information on grassland management as forcing. This requirement currently limits the applicability of DALEC-Grass to the areas with detailed management

data. The ACMv1 model (i.e. the module used to estimate GPP) used in DALEC-Grass does not consider the impact of plant water availability, and thus drought stress, on GPP. This likely has a limited effect on simulations in Scotland but DALEC-Grass can be updated if needed using a recently developed version of ACM that explicitly considers water cycling on estimation of GPP (Smallman and Williams, 2019). Furthermore, DALEC-Grass does not, at this stage, have a detailed description of the role of N for grass growth and C allocation. Because Easter Bush and Crichton are amply fertilised grasslands the results of this study are premised on non N-limited conditions. However, the lack of N cycling representation also means that soil C to N ratio and its role in litter and organic matter decomposition is not considered. The conversion of grazed biomass to C returned to the soil, in the form of excrement, depends on generic conversion factors but the assumption that all the daily-produced animal excrement is deposited on the soil is not realistic. Nevertheless, all livestock-related constants can be converted to parameters with appropriate respective priors, which can, in turn, be refined by CARDAMOM. Finally, in this study, we used field data from two sites in Scotland. These grasslands are representative of grasslands in the UK, and northwest Europe, but testing DALEC-Grass at grasslands across the world is needed for broader application.

4.4. Future development

Notwithstanding the aforementioned limitations, DALEC-Grass has a range of potential applications that vary from gap-filling time-series of C fluxes from micrometeorological towers to farm-level grassland C budgeting and validation of large-scale terrestrial ecosystem models. With appropriate development and testing the model can handle spatially resolved satellite-based data on LAI, which will allow the quantification of grassland productivity and C dynamics at landscape, regional and even national scales. To this end, DALEC-Grass will have to be developed in a way that allows the inference of management at grass-covered pixels of satellite images of the land's surface. Such a spatially-resolved version of DALEC-Grass, when used in CARDAMOM, will allow us to better understand how key factors such as livestock density and cutting intensity affect ecosystem productivity and C sequestration.

5. Conclusions

We demonstrated how a model of C dynamics linked by a model-data fusion framework to observations of LAI generated constrained analyses of grassland ecosystem functioning under management. The results of this study suggest that landscape grassland C cycling can be constrained using LAI data at relevant resolutions and accuracy. An initial parameter calibration using eddy flux data constrained key C cycle parameters, leading to a better understanding of grassland productivity and C sequestration capacity. Once this calibration was completed, assimilation of LAI data over time allowed the model to make robust estimates of the effects of grass grazing and cutting on net CO_2 exchanges. The data assimilation approach meant that the effects of parametric and observation uncertainties could be considered and quantified. We showed that the forecast uncertainty in our predictions was comparable to that of independent observations. We provide evidence that DALEC-Grass is a conceptually sound, structurally robust and computationally lightweight model. In the era of EO satellites, and the associated availability of swathes of data, the attributes of the model show its potential to provide in-depth monitoring of managed grasslands across temporal and spatial scales. Our aim is to realise this potential by further appropriate development and testing at landscape scales.

6. Acknowledgements

VM and MW devised the study concept. VM developed DALEC-Grass , implemented the MDF and undertook the analysis with support from all authors. Remaining authors provided data from the study sites. VM led the writing, with support from MW and LS. All authors contributed to the text. This study was supported by the Natural Environment Research Council (NERC) of the UK through the Soils Research to deliver Greenhouse Gas REmovals and Abatement Technologies (Soils-R-GGREAT) project, and the NERC GHG Programme GREENHOUSE project. This work was also part funded by the Scottish Government's Strategic Research Programme. We thank Anthony Bloom (JPL-NASA) for his support in development of CARDAMOM. We thank Tim Hill (University of Exeter) for access to eddy covariance instrumentation used at Crichton.

7. References

M Abdalla, A Hastings, D R Chadwick, D L Jones, C D Evans, M B Jones, R M Rees, and Pete Smith. Critical review of the impacts of grazing intensity on soil organic carbon storage and other soil quality indicators in extensively managed grasslands. *Agriculture, Ecosystems and Environment*, 253:62–81, feb 2018. doi: doi:10.1016/j.agee.2017.10.023.

Iftikhar Ali, Fiona Cawkwell, Edward Dwyer, Brian Barrett, and Stuart Green. Satellite remote sensing of grasslands: from observation to management. *Journal of Plant Ecology*, 9(6):649–671, dec 2016.

S. Asam, D. Klein, and S. Dech. Estimation of grassland use intensities based on high spatial resolution LAI time series. *International Archives of the Photogrammetry, Remote Sensing and Spatial Information Sciences - ISPRS Archives*, 40(7W3):285–291, 2015. ISSN 16821750. doi: 10.5194/isprsarchives-XL-7-W3-285-2015.

Josep Barba, Alejandro Cueva, Michael Bahn, Greg A. Barron-Gafford, Benjamin Bond-Lamberty, Paul J. Hanson, Aline Jaimes, Liisa Kulmala, Jukka Pumpanen, Russell L. Scott, Georg Wohlfahrt, and Rodrigo Vargas. Comparing ecosystem and soil respiration: Review and key challenges of tower-based and soil measurements. *Agricultural and Forest Meteorology*, 249(March 2017):434–443, 2018. ISSN 01681923. doi: 10.1016/j.agrformet.2017.10.028.

M. J. Bell, J. M. Cloy, C. F.E. Topp, B. C. Ball, A. Bagnall, R. M. Rees, and D. R. Chadwick. Quantifying N2O emissions from intensive grassland production: The role of synthetic fertilizer type, application rate, timing and nitrification inhibitors. *Journal of Agricultural Science*, 154(5):812–827, 2016. ISSN 14695146. doi: 10.1017/S0021859615000945.

H. Ben Touhami and G. Bellocchi. Bayesian calibration of the Pasture Simulation model (PaSim) to simulate European grasslands under water stress. *Ecological Informatics*, 30:356–364, 2015. doi: 10.1016/j.ecoinf.2015.09.009.

A A Bloom and M Williams. Constraining ecosystem carbon dynamics in a data-limited world: integrating ecological "common sense" in a modelâĂŞdata fusion framework. *Biogeosciences*, 12(5):1299–1315, jan 2015.

A Anthony Bloom, Jean-François Exbrayat, Ivar R van der Velde, Liang Feng, and Mathew Williams. The decadal state of the terrestrial carbon cycle: Global retrievals of terrestrial carbon allocation, pools, and residence times. *Proceedings of the National Academy of Sciences of the United States of America*, 113(5):1285–1290, feb 2016.

R.I. Bradley, R. Milne, J. Bell, A. Lilly, C. Jordan, and A. Higgins. A soil carbon and land use database for the United Kingdom. *Soil Use and Management*, 21(4):363–369, 2006. ISSN 02660032. doi: 10.1079/sum2005351.

Stephen P. Brooks and Andrew Gelman. General methods for monitoring convergence of iterative simulations)? *Journal of Computational and Graphical Statistics*, 7(4):434–455, 1998. ISSN 15372715. doi: 10.1080/10618600.1998.10474787.

J. F. Chang, N. Viovy, N. Vuichard, P. Ciais, T. Wang, A. Cozic, R. Lardy, A. I. Graux, K. Klumpp, R. Martin, and J. F. Soussana. Incorporating grassland management in ORCHIDEE: model description and evaluation at 11 eddy-covariance sites in Europe. *Geoscientific Model Development*, 6(6):2165–2181, 2013. ISSN 19919603. doi: 10.5194/gmd-6-2165-2013.

Jinfeng Chang, Philippe Ciais, Nicolas Viovy, Nicolas Vuichard, Benjamin Sultan, and Jean François Soussana. The greenhouse gas balance of European grasslands. *Global Change Biology*, 21(10):3748–3761, 2015. ISSN 13652486. doi: 10.1111/gcb.12998.

Jinfeng Chang, Philippe Ciais, Nicolas Viovy, Jean François Soussana, Katja Klumpp, and Benjamin Sultan. Future productivity and phenology changes in European grasslands for different warming levels: Implications for grassland management and carbon balance. *Carbon Balance and Management*, 12(1), 2017. ISSN 17500680. doi: 10.1186/s13021-017-0079-8.

Lajiao Chen and Lizhe Wang. Recent advance in earth observation big data for hydrology. *Big Earth Data*, 2(1):86–107, 2018. ISSN 2096-4471. doi: 10.1080/20964471.2018.1435072.

Wenqing Chen, Ding Huang, Nan Liu, Yingjun Zhang, Warwick B. Badgery, Xiaoya Wang, and Yue Shen. Improved grazing management may increase soil carbon sequestration in temperate steppe. *Scientific Reports*, 5:1–13, 2015. ISSN 20452322. doi: 10.1038/srep10892.

Siddhartha Chib and Edward Greenberg. Understanding the Metropolis-Hastings Algorithm Siddhartha Chib ; Edward Greenberg. *The American Statistician*, 49(4):327–335, 1995.

Richard T. Conant, Carlos E.P. Cerri, Brooke B. Osborne, and Keith Paustian. Grassland management impacts on soil carbon stocks: A new synthesis: A. *Ecological Applications*, 27(2):662–668, 2017. ISSN 19395582. doi: 10.1002/eap.1473.

COSMOS-UK. Cosmic-ray soil moisture monitoring network: Site data. `https://cosmos.ceh.ac.uk/Network`, 2019.

Rafael De Oliveira Silva, Luis Gustavo Barioni, Giampaolo Queiroz Pellegrino, and Dominic Moran. The role of agricultural intensification in Brazil's Nationally Determined Contribution on emissions mitigation. *Agricultural Systems*, 161(August 2017):102–112, 2018. ISSN 0308521X. doi: 10.1016/j.agsy.2018.01.003.

Pauline Dusseux, Xing Gong, Laurence Hubert-Moy, and Thomas Corpetti. Identification of grassland management practices from leaf area index time series. *Journal of Applied Remote Sensing*, 8(1):083559, 2014. ISSN 1931-3195. doi: 10.1117/1.JRS.8.083559.

Fiona Ehrhardt, Jean-Francois Soussana, Gianni Bellocchi, Peter Grace, Russel McAuliffe, Sylvie Recous, Renáta Sándor, Pete Smith, Val Snow, Massimiliano de Antoni Migliorati, Bruno Basso, Arti Bhatia, Lorenzo Brilli, Jordi Doltra, Christopher D Dorich, Luca Doro, Nuala Fitton, Sandro J Giacomini, Brian Grant, Matthew T Harrison, Stephanie K Jones, Miko U F Kirschbaum, Katja Klumpp, Patricia Laville, Joël Léonard, Mark Liebig, Mark Lieffering, Raphaël Martin, Raia S Massad, Elizabeth Meier, Lutz Merbold, Andrew D Moore, Vasileios Myrgiotis, Paul Newton, Elizabeth Pattey, Susanne Rolinski, Joanna Sharp, Ward N Smith, Lianhai Wu, and Qing Zhang. Assessing uncertainties in crop and pasture ensemble model simulations of productivity and N 2O emissions. *Global Change Biology*, 24(2):e603–e616, nov 2017. doi: http://doi.wiley.com/10.1111/gcb.13965.

Karl Heinz Erb, Thomas Kastner, Christoph Plutzar, Anna Liza S. Bais, Nuno Carvalhais, Tamara Fetzel, Simone Gingrich, Helmut Haberl, Christian Lauk, Maria Niedertscheider, Julia Pongratz, Martin Thurner, and Sebastiaan Luyssaert. Unexpectedly large impact of forest management

and grazing on global vegetation biomass. *Nature*, 553(7686):73–76, jan 2018. ISSN 14764687. doi: 10.1038/nature25138.

Th Foken and B. Wichura. Tools for quality assessment of surface-based flux measurements. *Agricultural and Forest Meteorology*, 78(1-2):83–105, 1996. ISSN 01681923. doi: 10.1016/0168-1923(95)02248-1.

Andrew Fox, Mathew Williams, Andrew D Richardson, David Cameron, Jeffrey H Gove, Tristan Quaife, Daniel Ricciuto, MARKUS REICHSTEIN, Enrico Tomelleri, Cathy M Trudinger, and Mark T Van Wijk. The REFLEX project: Comparing different algorithms and implementations for the inversion of a terrestrial ecosystem model against eddy covariance data. *Agricultural and Forest Meteorology*, 149(10):1597–1615, oct 2009.

Jonas Franke, Vanessa Keuck, and Florian Siegert. Assessment of grassland use intensity by remote sensing to support conservation schemes. *Journal for Nature Conservation*, 20(3):125–134, 2012. ISSN 16171381. doi: 10.1016/j.jnc.2012.02.001.

Pierre Friedlingstein, Matthew W. Jones, Michael O'Sullivan, Robbie M. Andrew, Judith Hauck, Glen P. Peters, Wouter Peters, Julia Pongratz, Stephen Sitch, Corinne Le Quéré, Orothee C.E. DBakker, Josep G. Canadell1, Philippe Ciais1, Robert B. Jackson, Peter Anthoni1, Leticia Barbero, Ana Bastos, Vladislav Bastrikov, Meike Becker, Laurent Bopp, Erik Buitenhuis, Naveen Chandra, Frédéric Chevallier, Louise P. Chini, Kim I. Currie, Richard A. Feely, Marion Gehlen, Dennis Gilfillan, Thanos Gkritzalis, Daniel S. Goll, Nicolas Gruber, Sören Gutekunst, Ian Harris, Vanessa Haverd, Richard A. Houghton, George Hurtt, Tatiana Ilyina, Atul K. Jain, Emilie Joetzjer, Jed O. Kaplan, Etsushi Kato, Kees Klein Goldewijk, Jan Ivar Korsbakken, Peter Landschützer, Siv K. Lauvset, Nathalie Lefèvre, Andrew Lenton, Sebastian Lienert, Danica Lombardozzi, Gregg Marland, Patrick C. McGuire, Joe R. Melton, Nicolas Metzl, David R. Munro, Julia E.M.S. Nabel, Shin Ichiro Nakaoka, Craig Neill, Abdirahman M. Omar, Tsuneo Ono, Anna Peregon, Denis Pierrot, Benjamin Poulter, Gregor Rehder, Laure Resplandy, Eddy Robertson, Christian Rödenbeck, Roland Séférian, Jörg Schwinger, Naomi Smith, Pieter P. Tans, Hanqin Tian, Bronte Tilbrook, Francesco N. Tubiello, Guido R. Van Der Werf, Andrew J. Wiltshire, and Sönke Zaehle. Global carbon budget 2019.

Earth System Science Data, 11(4):1783–1838, 2019. ISSN 18663516. doi: 10.5194/essd-11-1783-2019.

Andrew Gelman and Donald B. Rubin. Inference from iterative simulation using multiple sequences. *Statistical Science*, 7(4):457–472, 1992. ISSN 08834237. doi: 10.1214/ss/1177011136.

Liz Genever and Sue Buckingham. Planning grazing strategies for Better Returns. Technical report, Agriculture and Horticulture Development Board, UK, 2016.

David J Gibson. *Grasses and Grassland Ecology*. Oxford University Press, 2010. ISBN 0198529198. doi: 10.2989/10220111003703542. URL `http://www.tandfonline.com/doi/abs/10.2989/10220111003703542`.

T. G. Gilmanov, J. F. Soussana, L. Aires, V. Allard, C. Ammann, M. Balzarolo, Z. Barcza, C. Bernhofer, C. L. Campbell, A. Cernusca, A. Cescatti, J. Clifton-Brown, B. O.M. Dirks, S. Dore, W. Eugster, J. Fuhrer, C. Gimeno, T. Gruenwald, L. Haszpra, A. Hensen, A. Ibrom, A. F.G. Jacobs, M. B. Jones, G. Lanigan, T. Laurila, A. Lohila, G.Manca, B. Marcolla, Z. Nagy, K. Pilegaard, K. Pinter, C. Pio, A. Raschi, N. Rogiers, M. J. Sanz, P. Stefani, M. Sutton, Z. Tuba, R. Valentini, M. L. Williams, and G. Wohlfahrt. Partitioning European grassland net ecosystem CO2 exchange into gross primary productivity and ecosystem respiration using light response function analysis. *Agriculture, Ecosystems and Environment*, 121(1-2):93–120, 2007. ISSN 01678809. doi: 10.1016/j.agee.2006.12.008.

Marta Gómez Giménez, Rogier de Jong, Raniero Della Peruta, Armin Keller, and Michael E. Schaepman. Determination of grassland use intensity based on multi-temporal remote sensing data and ecological indicators. *Remote Sensing of Environment*, 198:126–139, 2017. ISSN 00344257. doi: 10.1016/j.rse.2017.06.003.

P. Gottschalk, M. Wattenbach, A. Neftel, J. Fuhrer, M. Jones, G. Lanigan, P. Davis, C. Campbell, J. F. Soussana, and P. Smith. The role of measurement uncertainties for the simulation of grassland net ecosystem exchange (NEE) in Europe. *Agriculture, Ecosystems and Environment*, 121(1-2):175–185, 2007. ISSN 01678809. doi: 10.1016/j.agee.2006.12.026.

Huadong Guo, Lizhe Wang, Fang Chen, and Dong Liang. Scientific big data and Digital Earth. *Chinese Science Bulletin*, 59(35):5066–5073, 2014. ISSN 18619541. doi: 10.1007/s11434-014-0645-3.

Yunqing Hao and Zhengwei He. Effects of grazing patterns on grassland biomass and soil environments in China: A meta-analysis. *PLoS ONE*, 14 (4):1–15, 2019. ISSN 19326203. doi: 10.1371/journal.pone.0215223.

Mario Herrero, Petr Havlík, Hugo Valin, An Notenbaert, Mariana C Rufino, Philip K Thornton, Michael Bluemmel, Franz Weiss, Delia Grace, and Michael Obersteiner. Biomass use, production, feed efficiencies, and greenhouse gas emissions from global livestock systems. *Proceedings of the National Academy of Sciences of the United States of America*, 110(52): 20888–20893, jan 2013.

Timothy Charles Hill, Edmund Ryan, and Mathew Williams. The use of CO 2 flux time series for parameter and carbon stock estimation in carbon cycle research. *Global Change Biology*, 18(1):179–193, 2012. ISSN 13541013. doi: 10.1111/j.1365-2486.2011.02511.x.

Tobias Houska, Philipp Kraft, Alejandro Chamorro-Chavez, and Lutz Breuer. SPOTting Model Parameters Using a Ready-Made Python Package. *PLoS ONE*, 10(12):e0145180–22, dec 2015. doi: https://doi.org/10.1371/journal.pone.0145180.

Bruce A Hungate, Edward B Barbier, Amy W Ando, Samuel P Marks, Peter B Reich, Natasja van Gestel, David Tilman, Johannes M H Knops, David U Hooper, Bradley J Butterfield, and Bradley J Cardinale. The economic value of grassland species for carbon storage. *Science Advances*, 3(4):e1601880, 2017.

William M Jolly, Ramakrishna Nemani, and Steven W Running. A generalized, bioclimatic index to predict foliar phenology in response to climate. *Global Change Biology*, 11(4):619–632, apr 2005.

Stephanie K Jones, Carole Helfter, Margaret Anderson, Mhairi Coyle, Claire Campbell, Daniela Famulari, Chiara Di Marco, Netty van Dijk, Y Sim Tang, Cairistiona F E Topp, Ralf Kiese, Reimo Kindler, Jan Siemens, Marion Schrumpf, Klaus Kaiser, Eiko Nemitz, Peter E Levy, Robert M Rees, Mark A Sutton, and Ute M Skiba. The nitrogen, carbon and greenhouse

gas budget of a grazed, cut and fertilised temperate grassland. *Biogeosciences*, 14(8):2069–2088, jan 2017.

Trevor F. Keenan, Eric Davidson, Antje M. Moffat, William Munger, and Andrew D. Richardson. Using model-data fusion to interpret past trends, and quantify uncertainties in future projections, of terrestrial ecosystem carbon cycling. *Global Change Biology*, 18(8):2555–2569, 2012. ISSN 13541013. doi: 10.1111/j.1365-2486.2012.02684.x.

Richard P. Kipling, Perttu Virkajärvi, Laura Breitsameter, Yannick Curnel, Tom De Swaef, Anne Maj Gustavsson, Sylvain Hennart, Mats Höglind, Kirsi Järvenranta, Julien Minet, Claas Nendel, Tomas Persson, Catherine Picon-Cochard, Susanne Rolinski, Daniel L. Sandars, Nigel D. Scollan, Leon Sebek, Giovanna Seddaiu, Cairistiona F.E. Topp, Stanislaw Twardy, Jantine Van Middelkoop, Lianhai Wu, and Gianni Bellocchi. Key challenges and priorities for modelling European grasslands under climate change. *Science of the Total Environment*, 566-567:851–864, 2016. ISSN 18791026. doi: 10.1016/j.scitotenv.2016.05.144.

S. Kuppel, P. Peylin, F. Maignan, F. Chevallier, G. Kiely, L. Montagnani, and A. Cescatti. Model-data fusion across ecosystems: From multisite optimizations to global simulations. *Geoscientific Model Development*, 7 (6):2581–2597, 2014. ISSN 19919603. doi: 10.5194/gmd-7-2581-2014.

Etienne Laliberté, Bill Shipley, David A. Norton, and David Scott. Which plant traits determine abundance under long-term shifts in soil resource availability and grazing intensity? *Journal of Ecology*, 100(3):662–677, 2012. ISSN 00220477. doi: 10.1111/j.1365-2745.2011.01947.x.

Mark A. Lee, Allison Todd, Mark A. Sutton, Mizeck G.G. Chagunda, David J. Roberts, and Robert M. Rees. A time-series of methane and carbon dioxide production from dairy cows during a period of dietary transition. *Cogent Environmental Science*, 3(1):1–14, 2017. ISSN 2331-1843. doi: 10.1080/23311843.2017.1385693. URL `http://doi.org/10.1080/23311843.2017.1385693`.

Xudong Li, Ding Guo, Chunping Zhang, Decao Niu, Hua Fu, and Changgui Wan. Contribution of root respiration to total soil respiration in a semi-arid grassland on the Loess Plateau, China. *Science of the Total Environment*,

627(768):1209–1217, 2018. ISSN 18791026. doi: 10.1016/j.scitotenv.2018.01.313.

Mengzhou Liu, Zhengwen Wang, Shanshan Li, Xiaotao Lü, Xiaobo Wang, and Xingguo Han. Changes in specific leaf area of dominant plants in temperate grasslands along a 2500-km transect in northern China. *Scientific Reports*, 7(1):1–9, 2017. ISSN 20452322. doi: 10.1038/s41598-017-11133-z.

Shaoxiu Ma, Romain Lardy, Anne Isabelle Graux, Haythem Ben Touhami, Katja Klumpp, Raphaël Martin, and Gianni Bellocchi. Regional-scale analysis of carbon and water cycles on managed grassland systems. *Environmental Modelling and Software*, 72:356–371, 2015. ISSN 18736726. doi: 10.1016/j.envsoft.2015.03.007.

Megan E. Mcsherry and Mark E. Ritchie. Effects of grazing on grassland soil carbon: A global review. *Global Change Biology*, 19(5):1347–1357, 2013. ISSN 13541013. doi: 10.1111/gcb.12144.

N. Meyer, G. Welp, and W. Amelung. The Temperature Sensitivity (Q10) of Soil Respiration: Controlling Factors and Spatial Prediction at Regional Scale Based on Environmental Soil Classes. *Global Biogeochemical Cycles*, 32(2):306–323, 2018. ISSN 19449224. doi: 10.1002/2017GB005644.

Karel Mokany, R John Raison, and Anatoly S Prokushkin. Critical analysis of root : shoot ratios in terrestrial biomes. *Global Change Biology*, 12:84–96, jan 2006. doi: http://doi.wiley.com/10.1111/j.1365-2486.2005.001043.x.

Vasileios Myrgiotis, Mathew Williams, Robert M Rees, Kate E Smith, Rachel E Thorman, and Cairistiona F E Topp. Model evaluation in relation to soil N2O emissions: An algorithmic method which accounts for variability in measurements and possible time lags. *Environmental Modelling & Software*, 84(C):251–262, 2016. doi: https://doi.org/10.1016/j.envsoft.2016.07.002.

Vasileios Myrgiotis, Mathew Williams, Cairistiona F E Topp, and Robert M Rees. Improving model prediction of soil N2O emissions through Bayesian calibration. *Science of The Total Environment*, 624:1467–1477, 2018. doi: https://doi.org/10.1016/j.scitotenv.2017.12.202.

Jouke Oenema, Saskia Burgers, Herman van Keulen, and Martin van Ittersum. Stochastic uncertainty and sensitivities of nitrogen flows on dairy

farms in The Netherlands. *Agricultural Systems*, 137:126–138, 2015. doi: 10.1016/j.agsy.2015.04.009.

AJ Parsons, J.S. Rowarth, and P.C.D Newton. Managing pasture for animals and soil carbon. *Proceedings of the New ...*, 71: 77–84, 2009. URL `http://www.grassland.org.nz/publications/nzgrassland{_}publication{_}70.pdf`.

G. Patenaude, R. Milne, M. Van Oijen, C. S. Rowland, and R. A. Hill. Integrating remote sensing datasets into ecological modelling: A Bayesian approach. *International Journal of Remote Sensing*, 29(5):1295–1315, 2008. ISSN 13665901. doi: 10.1080/01431160701736414.

Marc Peaucelle, Cédric Bacour, Philippe Ciais, Nicolas Vuichard, Sylvain Kuppel, Josep Peñuelas, Luca Belelli Marchesini, Peter D. Blanken, Nina Buchmann, Jiquan Chen, Nicolas Delpierre, Ankur R. Desai, Eric Dufrene, Damiano Gianelle, Cristina Gimeno-Colera, Carsten Gruening, Carole Helfter, Lukas Hörtnagl, Andreas Ibrom, Richard Joffre, Tomomichi Kato, Thomas E. Kolb, Beverly Law, Anders Lindroth, Ivan Mammarella, Lutz Merbold, Stefano Minerbi, Leonardo Montagnani, Ladislav Šigut, Mark Sutton, Andrej Varlagin, Timo Vesala, Georg Wohlfahrt, Sebastian Wolf, Dan Yakir, and Nicolas Viovy. Covariations between plant functional traits emerge from constraining parameterization of a terrestrial biosphere model. *Global Ecology and Biogeography*, 28(9):1351–1365, 2019. ISSN 14668238. doi: 10.1111/geb.12937.

Philippe Peylin, Cédric Bacour, Natasha MacBean, Sébastien Leonard, Peter Rayner, Sylvain Kuppel, Ernest Koffi, Abdou Kane, Fabienne Maignan, Frédéric Chevallier, Philippe Ciais, and Pascal Prunet. A new stepwise carbon cycle data assimilation system using multiple data streams to constrain the simulated land surface carbon cycle. *Geoscientific Model Development*, 9(9):3321–3346, 2016. ISSN 19919603. doi: 10.5194/gmd-9-3321-2016.

Nicolas Puche, Nimai Senapati, Christophe R. Flechard, Katia Klumpp, Miko U.F. Kirschbaum, and Abad Chabbi. Modeling carbon and water fluxes of managed grasslands: Comparing flux variability and net carbon budgets between grazed and mowed systems. *Agronomy*, 9(4):10–12, 2019. ISSN 20734395. doi: 10.3390/agronomy9040183.

S. M. Punalekar, A. Verhoef, T. L. Quaife, D. Humphries, L. Bermingham, and C. K. Reynolds. Application of Sentinel-2A data for pasture biomass monitoring using a physically based radiative transfer model. *Remote Sensing of Environment*, 218(October 2017):207–220, 2018. ISSN 00344257. doi: 10.1016/j.rse.2018.09.028.

Aiming Qi, Philip J Murray, and Goetz M Richter. Modelling productivity and resource use efficiency for grassland ecosystems in the UK. *European Journal of Agronomy*, 89:148–158, sep 2017.

Aiming Qi, Robert A. Holland, Gail Taylor, and Goetz M. Richter. Grassland futures in Great Britain - Productivity assessment and scenarios for land use change opportunities. *Science of the Total Environment*, 634:1108–1118, 2018. doi: 10.1016/j.scitotenv.2018.03.395.

Hampapuram K. Ramapriyan and Kevin J. Murphy. Collaborations and Partnerships in NASA's Earth Science Data Systems. *Data Science Journal*, 16(Nasa):1–7, 2017. doi: 10.5334/dsj-2017-051.

Michael R. Raupach, P. J. Rayner, D. J. Barrett, R. S. Defries, M. Heimann, D. S. Ojima, S. Quegan, and C. C. Schmullius. Model-data synthesis in terrestrial carbon observation: Methods, data requirements and data uncertainty specifications. *Global Change Biology*, 11(3):378–397, 2005. ISSN 13541013. doi: 10.1111/j.1365-2486.2005.00917.x.

Markus Reichstein, Eva Falge, Dennis Baldocchi, Dario Papale, Marc Aubinet, Paul Berbigier, Christian Bernhofer, Nina Buchmann, Tagir Gilmanov, André Granier, Thomas Grünwald, Katka Havránková, Hannu Ilvesniemi, Dalibor Janous, Alexander Knohl, Tuomas Laurila, Annalea Lohila, Denis Loustau, Giorgio Matteucci, Tilden Meyers, Franco Miglietta, Jean Marc Ourcival, Jukka Pumpanen, Serge Rambal, Eyal Rotenberg, Maria Sanz, John Tenhunen, Günther Seufert, Francesco Vaccari, Timo Vesala, Dan Yakir, and Riccardo Valentini. On the separation of net ecosystem exchange into assimilation and ecosystem respiration: Review and improved algorithm. *Global Change Biology*, 11(9):1424–1439, 2005. ISSN 13541013. doi: 10.1111/j.1365-2486.2005.001002.x.

Andrew Revill, A Anthony Bloom, and Mathew Williams. Impacts of reduced model complexity and driver resolution on cropland ecosystem photosynthesis estimates. *Field Crops Research*, 187:74–86, feb 2016.

J. J. Reyes, C. L. Tague, R. D. Evans, and J. C. Adam. Assessing the Impact of Parameter Uncertainty on Modeling Grass Biomass Using a Hybrid Carbon Allocation Strategy. *Journal of Advances in Modeling Earth Systems*, 9(8):2968–2992, 2017. ISSN 19422466. doi: 10.1002/2017MS001022.

Susanne Rolinski, Christoph Müller, Jens Heinke, Isabelle Weindl, Anne Biewald, Benjamin Leon Bodirsky, Alberte Bondeau, Eltje R Boons-Prins, Alexander F Bouwman, Peter A Leffelaar, Johnny A te Roller, Sibyll Schaphoff, and Kirsten Thonicke. Modeling vegetation and carbon dynamics of managed grasslands at the global scale with LPJmL 3.6. *Geoscientific Model Development*, 11(1):429–451, 2018.

Renáta Sándor, Fiona Ehrhardt, Peter Grace, Sylvie Recous, Pete Smith, Val Snow, Jean François Soussana, Bruno Basso, Arti Bhatia, Lorenzo Brilli, Jordi Doltra, Christopher D. Dorich, Luca Doro, Nuala Fitton, Brian Grant, Matthew Tom Harrison, Miko U.F. Kirschbaum, Katja Klumpp, Patricia Laville, Joel Léonard, Raphaël Martin, Raia Silvia Massad, Andrew Moore, Vasileios Myrgiotis, Elizabeth Pattey, Susanne Rolinski, Joanna Sharp, Ute Skiba, Ward Smith, Lianhai Wu, Qing Zhang, and Gianni Bellocchi. Ensemble modelling of carbon fluxes in grasslands and croplands. *Field Crops Research*, 252(March):107791, 2020. ISSN 03784290. doi: 10.1016/j.fcr.2020.107791.

Marko Scholze, Michael Buchwitz, Wouter Dorigo, Luis Guanter, and Shaun Quegan. Reviews and syntheses: Systematic Earth observations for use in terrestrial carbon cycle data assimilation systems. *Biogeosciences*, 14(14): 3401–3429, jan 2017.

T L Smallman, J F Exbrayat, M Mencuccini, A A Bloom, and M Williams. Assimilation of repeated woody biomass observations constrains decadal ecosystem carbon cycle uncertainty in aggrading forests. *Journal of Geophysical Research: Biogeosciences*, 122(3):528–545, 2017.

Thomas Lukas Smallman and Mathew Williams. Description and validation of an intermediate complexity model for ecosystem photosynthesis and evapotranspiration: ACM-GPP-ETv1. *Geoscientific Model Development*, 12(6):2227–2253, 2019. ISSN 19919603. doi: 10.5194/gmd-12-2227-2019.

H. J. Smit, M. J. Metzger, and F. Ewert. Spatial distribution of grassland

productivity and land use in Europe. *Agricultural Systems*, 98(3):208–219, 2008. ISSN 0308521X. doi: 10.1016/j.agsy.2008.07.004.

Pete Smith, Fabrizio Albanito, Madeleine Bell, Jessica Bellarby, Sergey Blagodatskiy, Arindam Datta, Marta Dondini, Nuala Fitton, Helen Flynn, Astley Hastings, Jon Hillier, Edward O. Jones, Matthias Kuhnert, Dali R. Nayak, Mark Pogson, Mark Richards, Gosia Sozanska-Stanton, Shifeng Wang, Jagadeesh B. Yeluripati, Emily Bottoms, Chris Brown, Jenny Farmer, Diana Feliciano, Cui Hao, Andy Robertson, Sylvia Vetter, Hon Man Wong, and Jo Smith. Systems approaches in global change and biogeochemistry research. *Philosophical Transactions of the Royal Society B: Biological Sciences*, 367(1586):311–321, 2012. ISSN 14712970. doi: 10.1098/rstb.2011.0173.

V. O. Snow, C. A. Rotz, A. D. Moore, R. Martin-Clouaire, I. R. Johnson, N. J. Hutchings, and R. J. Eckard. The challenges - and some solutions - to process-based modelling of grazed agricultural systems. *Environmental Modelling and Software*, 62:420–436, 2014. ISSN 13648152. doi: 10.1016/j.envsoft.2014.03.009.

Lynn E. Sollenberger, Marta M. Kohmann, Jose C.B. Dubeux, and Maria L. Silveira. Grassland management affects delivery of regulating and supporting ecosystem services. *Crop Science*, 59(2):441–459, 2019. ISSN 14350653. doi: 10.2135/cropsci2018.09.0594.

Jean François Soussana and Gilles Lemaire. Coupling carbon and nitrogen cycles for environmentally sustainable intensification of grasslands and crop-livestock systems. *Agriculture, Ecosystems and Environment*, 190:9–17, 2014. ISSN 01678809. doi: 10.1016/j.agee.2013.10.012.

Marcel van Oijen. Bayesian Methods for Quantifying and Reducing Uncertainty and Error in Forest Models. *Current Forestry Reports*, 3(4):269–280, 2017. ISSN 21986436. doi: 10.1007/s40725-017-0069-9.

Marcel van Oijen, Zoltán Barcza, Roberto Confalonieri, Panu Korhonen, György Kröel-Dulay, Eszter Lellei-Kovács, Gaëtan Louarn, Frédérique Louault, Raphaël Martin, Thibault Moulin, Ermes Movedi, Catherine Picon-Cochard, Susanne Rolinski, Nicolas Viovy, Stephen Björn Wirth, and Gianni Bellocchi. Incorporating biodiversity into biogeochemistry

models to improve prediction of ecosystem services in temperate grasslands: Review and roadmap. *Agronomy*, 10(2), 2020. ISSN 20734395. doi: 10.3390/agronomy10020259.

Don van Ravenzwaaij, Pete Cassey, and Scott D. Brown. A simple introduction to Markov Chain MonteâĂŞCarlo sampling. *Psychonomic Bulletin and Review*, 25(1):143–154, 2018. ISSN 15315320. doi: 10.3758/s13423-016-1015-8.

Mark T. Van Wijk and Mathew Williams. Optical instruments for measuring leaf area index in low vegetation: Application in arctic ecosystems. *Ecological Applications*, 15(4):1462–1470, 2005. ISSN 10510761. doi: 10.1890/03-5354.

Françoise Vertès, Luc Delaby, Katia Klumpp, and Juliette Bloor. C-N-P Uncoupling in Grazed Grasslands and Environmental Implications of Management Intensification. *Agroecosystem Diversity*, pages 15–34, 2018. doi: 10.1016/b978-0-12-811050-8.00002-9.

Nicolas Vuichard, Philippe Ciais, Nicolas Viovy, Pierluigi Calanca, and Jean-François Soussana. Estimating the greenhouse gas fluxes of European grasslands with a process-based model: 2. Simulations at the continental level. *Global Biogeochemical Cycles*, 21(1):n/a–n/a, 2007. ISSN 08866236. doi: 10.1029/2005GB002612.

Ying Ping Wang, Cathy M. Trudinger, and Ian G. Enting. A review of applications of model-data fusion to studies of terrestrial carbon fluxes at different scales. *Agricultural and Forest Meteorology*, 149(11):1829–1842, 2009. ISSN 01681923. doi: 10.1016/j.agrformet.2009.07.009.

Mathew Williams, Edward B. Rastetter, David N. Fernandes, Michael L. Goulden, Gaius R. Shaver, and Loretta C. Johnson. Predicting gross primary prodctivity in terrestrial ecosystems. *Ecological Applications*, 7(3): 882–894, 1997.

Fred Worrall and Gareth D. Clay. The impact of sheep grazing on the carbon balance of a peatland. *Science of the Total Environment*, 438:426–434, 2012. ISSN 00489697. doi: 10.1016/j.scitotenv.2012.08.084. URL `http://dx.doi.org/10.1016/j.scitotenv.2012.08.084`.

Jiangzhou Xia, Wenping Yuan, Ying Ping Wang, and Quanguo Zhang. Adaptive Carbon Allocation by Plants Enhances the Terrestrial Carbon Sink. *Scientific Reports*, 7(1):1–11, 2017. ISSN 20452322. doi: 10.1038/s41598-017-03574-3.

Jingfeng Xiao, Kenneth J Davis, Nathan M Urban, and Klaus Keller. Uncertainty in model parameters and regional carbon fluxes: A model-data fusion approach. *Agricultural and Forest Meteorology*, 189-190:175–186, 2014.

Dandan Xu and Xulin Guo. Some Insights on Grassland Health Assessment Based on Remote Sensing. *Sensors*, 15(2):3070–3089, 2015. ISSN 1424-8220. doi: 10.3390/s150203070.

Shuxia Zheng, Wenhuai Li, Zhichun Lan, Haiyan Ren, and Kaibo Wang. Functional trait responses to grazing are mediated by soil moisture and plant functional group identity. *Scientific Reports*, 5(December):1–12, 2015. ISSN 20452322. doi: 10.1038/srep18163. URL `http://dx.doi.org/10.1038/srep18163`.

Supplementary material

Table 5: DALEC-Grass parameters. Description, units and calibration results.

Code	Description	Unit	Prior_{min}	Prior_{max}	Posterior_{mean}	Posterior_{SD}	MAP	Prior length reduction (%)
P1	Decomposition rate	fraction d^{-1}	1.00e-05	0.3	0.06	0.03	0.08	97
P2	Fraction of GPP that is respired	-	0.4	0.51	0.4427	0.0298	0.4158	3
P3	GSI sensitivity for leaf growth	-	0.75	9	3.968	0.767	4.637	61
P4	NPP belowground allocation	-	0.01	1	0.330	0.068	0.352	60
P5	Maximum GSI for leaf turnover	-	1.00e-07	3	0.214	0.230	0.173	50
P6	Turnover rate of roots	fraction d^{-1}	1.00e-06	0.1	3.45e-03	1.98e-03	5.38e-03	91
P7	Turnover rate of litter	fraction d^{-1}	1.00e-06	0.1	4.39e-03	2.66e-03	3.07e-03	90
P8	Turnover rate of soil organic matter	fraction d^{-1}	1.00e-10	0.01	3.84e-05	2.75e-05	2.44e-06	99
P9	Temperature Q10 factor	-	0.008	0.15	0.0416	0.0162	0.0418	57
P10	Photosynthetic N use efficiency (PNUE)	g C per g N per leaf m^2 per day	7	25	15	3	18	31
P11	Maximum GSI for labile/stem turnover	-	0.0001	2	0.634	0.137	0.603	68
P12	Minimum GSI temperature threshold	K	225	330	251	16	264	27
P13	Maximum GSI temperature threshold	K	225	330	304	20	303	17
P14	Minimum GSI photoperiod threshold	seconds	3600	30000	12283	5191	6892	23
P15	Leaf Mass C per Area (LMCA)	g C per m^2 of leaf	20	60	46	6	46	56
P16	Initial C in stem/labile pool	g C m^{-2}	1	300	151	75	52	4
P17	Initial C in foliar pool	g C m^{-2}	1	300	132	68	43	13
P18	Initial C in roots pool	g C m^{-2}	1	5000	893	800	284	40
P19	Initial C in litter pool	g C m^{-2}	1	5000	793	561	486	52
P20	Maximum GSI photoperiod threshold	seconds	3600	64800	31917	6262	28880	42
P21	Minimum GSI VPD threshold	Pa	1	5500	1209	929	186	27
P22	Maximum GSI VPD threshold	Pa	1	5500	3376	1156	1457	16
P23	Critical GPP for LAI increase	g C m^{-2} d^{-1}	1.00e-05	1	0.30	0.13	0.26	53
P24	GSI sensitivity for leaf senescence	-	0.96	1	0.99	0.00	1.00	52
P25	GSI growing stage indicator	-	0.3	3	1.27	0.13	1.13	82
P26	Initial GSI value	-	0.5	3	1.61	0.23	1.83	61
P27	Minimum vegetation DM for grazing	kg DM ha^{-1}	500	2000	995	197	1114	30
P28	Minimum vegetation DM for cutting	kg DM ha^{-1}	1000	6000	3232	611	2896	52
P29	Leaf to stem allocation parameter	-	0.05	0.9	0.61	0.11	0.66	45
P30	Initial C in SOM pool	g C m^{-2}	5000	15000	9912	2513	9240	31
P31	DM demand (as % of animal weight)	-	0.01	0.03	0.02	0.01	0.03	2
P32	Post grazing labile/stem loss	-	0.001	0.75	0.16	0.06	0.19	67
P33	Post cutting labile/stem loss	-	0.001	0.75	0.18	0.15	0.08	34

GSI: Growing Season Index, VPD: Vapour Pressure Deficit, SOM: Soil Organic Matter,
DM: Dry Matter, GPP: Gross Primary Productivity, NPP: Net Primary Productivity
MAP: Maximum a posteriori probability estimate
Prior length reduction: 100*(1-(posterior_{max}-posterior_{min})/(prior_{max}-prior_{min}))
Estimates for the prior range for parameter P30 come from (Bradley et al., 2006)

Chain convergence assessment

The Gelman-Rubin potential scale reduction factor (PSRF) was calculated using the following equations :

$$B = \frac{N}{M-1}\Sigma_{m=1}^{M}(\overline{\theta_m} - \overline{\theta})^2 \tag{7}$$

$$W = \frac{1}{M}\Sigma_{m=1}^{M}\sigma_m^2 \tag{8}$$

$$\overline{V} = \frac{N-1}{N}W + \frac{M+1}{MN}B \tag{9}$$

$$PSRF = \sqrt{\frac{\overline{V}}{W}} \tag{10}$$

where θ is a model parameter, σ^2 is the variance, M is the number of chains and N is the length of each chain. A PSRF $\approx$ 1 shows that chain convergence was achieved. The use of EDCs in CARDAMOM means that N was not the same for all chains. For this reason we used the last 10000 values retrieved by the MH algorithm for each chain to calculate the PSRF. The PSRF for each parameter as estimated from results from the calibration period (2002-2004) are presented in Figure 9.

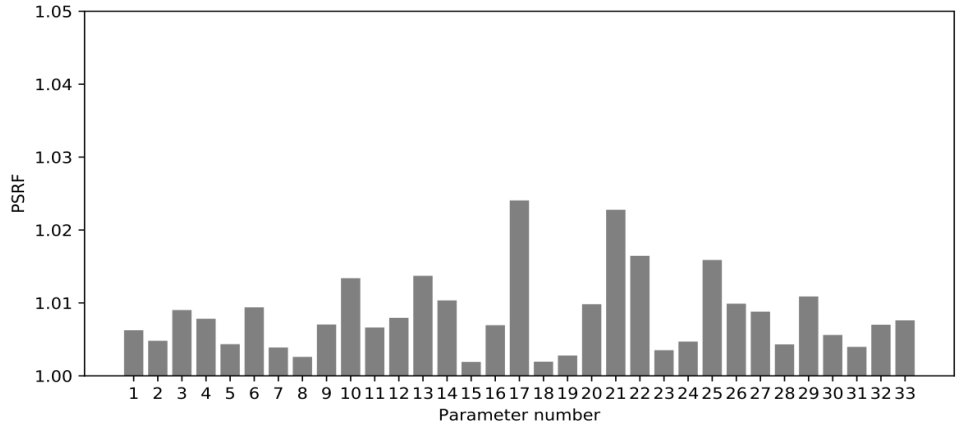

Figure 9: Estimated potential scale reduction factor (PSRF) for each model parameter after parameter calibration. The names (and other information) of each model parameter number are presented in Table 5

.

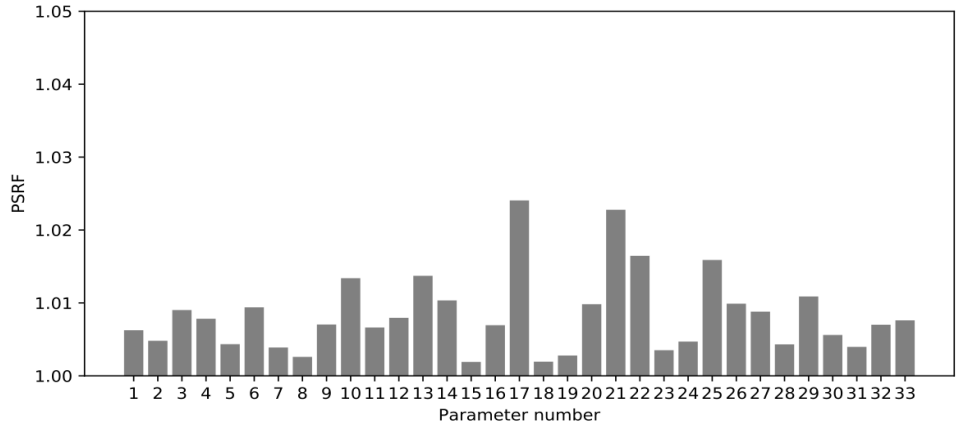

Figure 9: Estimated potential scale reduction factor (PSRF) for each model parameter after parameter calibration. The names (and other information) of each model parameter number are presented in Table 5

.